Drift Problems in the Automatic Analysis of Gamma-Ray Spectra Using Associative Memory Algorithms

P. Olmos, J. C. Diaz, J. M. Perez, P. Aguayo, P. Gomez, and V. Rodellar

Abstract—**Perturbations affecting nuclear radiation spectrometers during their operation frequently spoil the accuracy of automatic analysis methods. One of the problems usually found in practice refers to fluctuations in the spectrum gain and zero, produced by drifts in the detector and nuclear electronics. The pattern acquired in these conditions may be significantly different from that expected with stable instrumentation, thus complicating the identification and quantification of the radionuclides present in it. In this work, the performance of Associative Memory algorithms when dealing with spectra affected by drifts is explored considering a linear energy-calibration function. The formulation of the extended algorithm, constructed to quantify the possible presence of drifts in the spectrometer, is deduced and the results obtained from its application to several practical cases are commented.**

I. Introduction

An alternative method of automatic radiation spectra analysis, based on the use of a simple neural network algorithm known as linear associative memory, was presented in recent publications [1], [2]. In this scheme, the identification and quantification of the possible radioisotopes present in a given spectrum is carried out by obtaining the linear combination of single radionuclide spectra that optimally fits the pattern under study. Its theoretical and practical utility has been demonstrated when no extreme accuracy is needed and quite stable spectrometers are used.

One of the most significant problems found when analyzing radiation spectra is related with the stability of the nuclear instrumentation (detector and electronics) during long periods of time. Unfortunately, in many situations, the spectroscopic measurements exhibit drifts which may become clearly visible if the system is working in uncontrolled environments, such as under large temperature fluctuations or with excessively high count rates. These drifts affect the isotope recognition and quantification process, both in manual and (more deeply) in automatic mode.

In the classical treatment, several methods have been developed to correct the negative effects of the instrumentation drifts. These techniques try to restore the pattern by using complicated feedbacks (most of them based on the determination of the shiftings occurred in the position of some calibration peaks), implemented either at hardware [3]–[5] or software [6], [7] levels.

Taking into account the foundations of the associative memory algorithm, it is easy to realize that the application of those stabilization methods does not constitute a suitable option for correcting the bad response which is obtained from the algorithm with unstable instrumentation. It will be shown in this paper that these problems can be properly treated without considering other calibration patterns apart from the reference spectra used in the "training phase" [1]. The purpose of the extended algorithm is not strictly to correct the deviations produced by the instrument drift, but to find out their possible presence quantifying the main variables involved in them. Its successful performance in simulated and real cases will be demonstrated.

II. Theoretical Treatment

The mathematical treatment of the drifts occurred in nuclear instrumentation, within the associative memory schema, is very dependent upon the relation between the actual photon energy and the channel assigned to the pulse produced by the analog electronics, as a consequence of the interaction of the photon with the detector. This relation (energy-calibration function) defines the mathematical representation of the drifts that the algorithm takes into account.

Let us consider the basic modelling of this calibration function: the channel energy (x) assigned to the photon is related to its energy (E) by means of the following [8]:

$$x = aE + b, \tag{1}$$

a and b being the spectrum gain and zero, respectively.

That state in which $a = a_0$ and $b = b_0$ will be defined as the reference state and the spectra obtained in these conditions, represented as $s(x, a = a_0, b = b_0)$, correspond to the "drift-free" reference spectra. Any deviation from this state found in other measurement can be considered as a fluctuation in the parameters a and b, the "drifted" spectrum being represented as $s(x, a = a_0 +$

Manuscript received February 3, 1992; revised February 9, 1993.

P. Olmos, J. C. Diaz, J. M. Perez, and P. Aguayo are with CIEMAT, Avda. Complutense 22, 28040 Madrid, Spain.

P. Gomez and V. Rodellar are with Facultad de Informatica, 28660 Boadilla del Monte, Madrid, Spain.

IEEE Log Number 9400585.

$\Delta a, b = b_0 + \Delta b$). Both patterns are related by means of a Taylor's expansion

$$s(x, a_0 + \Delta a, b_0 + \Delta b) = s(x, a_0, b_0) + \frac{\partial s(x, a_0, b_0)}{\partial a} \Delta a + \frac{\partial s(x, a_0, b_0)}{\partial b} \Delta b + \cdots \quad (2)$$

Remembering that

$$\frac{\partial s(x, a_0, b_0)}{\partial a} = \frac{\partial s(x, a_0, b_0)}{\partial x} \frac{\partial x}{\partial a} = \frac{\partial s(x, a_0, b_0)}{\partial x} E \quad (3)$$

and

$$\frac{\partial s(x, a_0, b_0)}{\partial b} = \frac{\partial s(x, a_0, b_0)}{\partial x} \frac{\partial x}{\partial b} = \frac{\partial s(x, a_0, b_0)}{\partial x} \quad (4)$$

we arrive at the following result:

$$s(x, a_0 + \Delta a, b_0 + \Delta b) = s(x, a_0, b_0) + s'(x, a_0, b_0) \cdot E(x, a_0, b_0)\Delta a + s'(x, a_0, b_0)\Delta b + \cdots, \quad (5)$$

$s'(x, a_0, b_0)$ being the partial derivative of the reference spectra with respect to the variable representing the energy channels (x).

Under the hypothesis of linearity, it is seen that the effects of the drifts can be represented by a new function, which is deduced from a linear combination of the drift-free spectrum plus its derivatives multiplied by powers of Δa and Δb. This elemental mathematical technique allows one to analyze the drifted spectrum, as well as to find Δa and Δb, just by taking into account the derivatives of the spectra used to calibrate the instrument. The higher the order of this expansion, the more acute deviations can be properly treated.

III. Practical Implementation

In this section we will describe a simple implementation of these ideas, based on the automatic spectrum analysis method extensively described in [2]. The introduction of the ability to deal with (not too extreme) perturbations in the gain and zero is carried out through the following steps:

1) The reference spectra of the k isotopes which are expected to be found in the mixture are taken during the calibration, assuming for these reference spectra that $a = 1$ and $b = 0$.
2) The reference base, formed by these k primary spectra, is extended by adding the corresponding Taylor terms (defined by successive derivatives of the original patterns) up to desired order. Let us assume that we consider the pth order; thus, $2p$ new patterns are then associated to each reference isotope (p spectra for Δa and p for Δb).
3) These patterns, plus the original spectrum, are arranged in a matrix X having $(2p + 1) \times k$ columns and N rows (N being the number of channels).
4) Finally, the pseudoinverse matrix of X is found following an adaptive algorithm well explained elsewhere [9]. Once this matrix has been formed, the analysis is performed following the technique described in [2]. This is based essentially on finding the different projections of the vector representing the unknown spectrum on the vectorial subspace defined by the vectors (spectra) of the reference base. The inclusion of the capability of dealing with instrument perturbations is then equivalent to extend the dimensionality of this subspace by adding those vectors derived from the expansion terms.

In this way, the application of the pseudoinverse matrix to the unknown mixture of reference isotopes, affected by unpredictable perturbations, leads not only to the determination of the relative concentrations of those elements present in the sample, but also to estimations of Δa and Δb.

IV. Experimental Results

The ability of the method to deal with perturbations in the instrument response has been studied in several cases. The results obtained indicate that the improvement achieved with this extended algorithm becomes important when relatively severe drifts are present in the spectrum.

A. Simulated Drifts

Firstly, we will deal with those situations in which small differences in the spectrometer performance are encountered during long periods of time, the usual case when fine instrumentation is used. In these conditions, the operating characteristics may suffer deviations from the calibration ones (done time ago), although remaining essentially constant during the acquisition.

To study this situation, we have used spectra taken with a NaI detector, not affected by any kind of drift neither during calibration nor in operation. They were intentionally deformed in shape by introducing different values of the parameters a and b, according to the expression (1). Four isotopes, ^{133}Ba, ^{137}Cs, ^{60}Co and ^{22}Na, formed the calibration base and the patterns produced by several combinations of them were recorded while the instrument worked in normal conditions, carefully monitored during the acquisition. These undistorted spectra ($a = 1$, $b = 0$) were analyzed by the standard Associative Memory with good results, obtaining a complete identification and quantification of their components, as explained in [2]. The extended matrix X, considering those terms of the Taylor expansion corresponding to each isotope up to the order 2, yielded the same quantification when applied to drift-free spectra.

If new values of a and b are artificially introduced in these patterns, thus simulating perturbations occurred during the long term operation, spectra like the one plotted in Fig. 1(a) constitute the new input to the Associative Memory instead of that of Fig. 1(b). The first

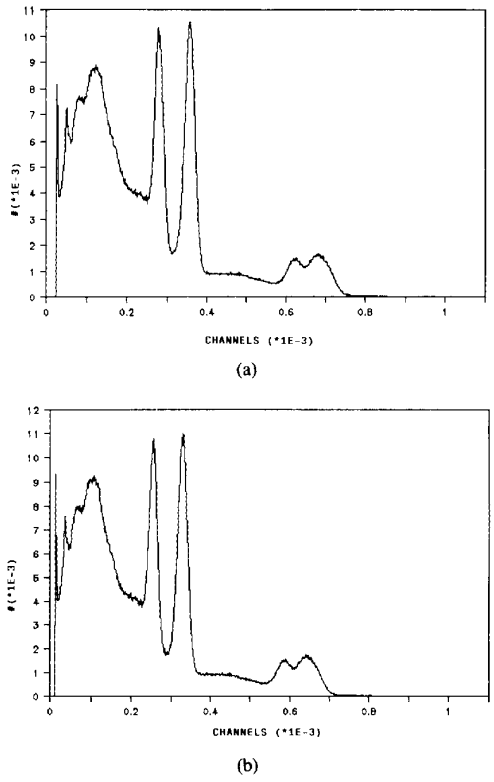

Fig. 1. (a) Spectrum formed by a mixture of ^{60}Co, ^{22}Na and ^{137}Cs, artificially deformed by an 8 channels shift and a variation in gain of 4%. (b) The spectrum of Fig. 1(a) taken under reference conditions.

spectrum, evidently different from what would be expected if no drift existed in the instrument, can not be properly analyzed with the standard matrix, which leads to meaningless conclusions. However, the extended matrix is able to identify and quantify the components present in this kind of patterns, the results remaining essentially similar (within a factor greater than 95%) to that obtained for the drift-free patterns, as can be seen in Tables I and II, where the isotope quantifications found for different values of Δa and Δb are presented. These results are acceptably accurate for deviations in gain as large as 5 per cent and shiftings in the origin smaller than 15 channels (the spectra had 1024 channels).

Once the performance of the recognition algorithm has been studied for "long-term" drifts, those cases in which the changes are produced during the acquisition period will be explored. This is not a rare case mainly when using spectrometers involving PM tubes, which may suffer small perturbations while they are detecting. The net effect of this phenomenon is to broaden the individual peaks of the patterns produced by the equipment.

On the basis of the linearity assumption inherent in the extension of the original method, it is easy to realize that this problem is reduced to the superposition of a set of elemental drifts of the type discussed before, each one occurred during a short period of time. Thus, the final Δa and Δb can be considered as the addition of the fluctuations associated to each elemental perturbation the technique keeps, in principle, its validity range.

TABLE I

Isotope	Δb					
	+2	−2	+8	−8	+15	−15
^{133}Ba	0	0	0	0	0	0
^{137}Cs	0	0	0	0	0	0
^{60}Co	0.4745	0.4745	0.4745	0.4754	0.4741	0.3891
^{22}Na	0.6059	0.6059	0.6059	0.6046	0.6052	0.5013
Δa	0	0	0	0	0	0
Δb	1.96	−1.95	8.01	−7.70	14.91	−14.02

Results of the analysis performed on a mixture of ^{60}Co and ^{22}Na assuming a drift in b, whereas the gain a was maintained constant (= 1). Reference quantities were: 0.4745 of ^{60}Co and 0.6059 of ^{22}Na. The top row shows the values of Δb assumed in the measurement process. The two bottom rows give the estimated values for the drifts.

TABLE II

Isotope	Δa					
	+1%	−1%	+2%	−2%	+4%	−4%
^{133}Ba	0	0	0	0	0	0
^{137}Cs	0	0	0	0	0	0
^{60}Co	0.4750	0.4750	0.4752	0.4754	0.4759	0.4863
^{22}Na	0.6055	0.6056	0.6061	0.6058	0.6060	0.6175
Δa	1.01	−0.99	1.90	−2.05	3.90	−4.16
Δb	0	0	0	0	0	0

Results of the analysis performed on a mixture of ^{60}Co and ^{22}Na assuming a drift in a, whereas the offset b was maintained constant (= 0). Reference quantities were: 0.4745 of ^{60}Co and 0.6059 of ^{22}Na. The top row shows the values of Δa assumed in the measurement process. The two bottom rows show the estimated values for the drifts.

To give quantitative evidence of the influence that this phenomenon has on the final output, we have constructed a reference base containing 16 simulated elements defined by 1024 bins patterns with several peaks. After training the algorithm with these spectra, plus their perturbation terms, an acquisition affected by small changes has been simulated for one of the reference spectra. This simulation was accomplished by assuming random variations of the gain and zero and deforming the pattern according with these perturbations, uniformly distributed in the intervals $[-\Delta a, \Delta a]$ and $[-\Delta b, \Delta b]$, respectively. Fig. 2 shows a representation of this situation. Each line corresponds to an elemental spectrum formed in the conditions defined by a given value of the gain and zero, randomly generated inside the before intervals; the pattern named "superposition" reflects the (normalized) addition of all these shapes. This last one should be compared with the outer pattern, the one present in the reference base. The broadening of the peaks due to this "on-line" drifts is clearly visible.

Table III gives the maximum relative deviation obtained in the analysis of this case, as a function of the gain and zero variations. Those cases signaled with "—" imply excessive large values of the rejection coefficient (defined as the projection of the unknown spectrum on a vector normal to the reference subspace [2]) and should, there-

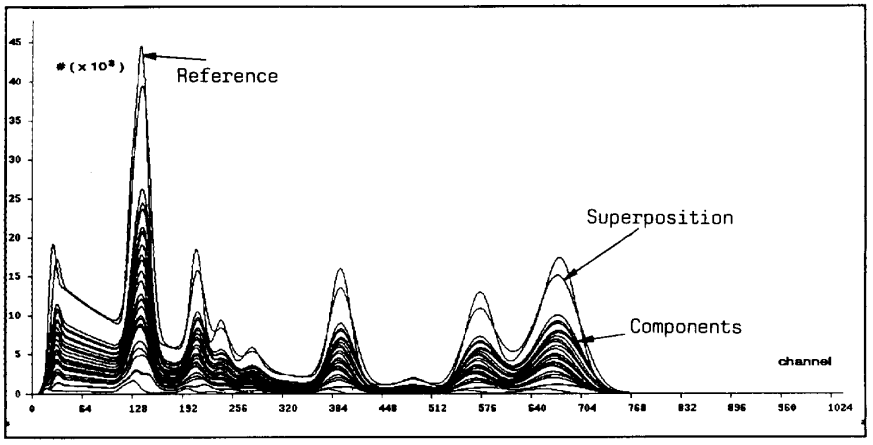

Fig. 2. Composite normalized spectrum resulting from the superposition of several spectra forming with different values of (a) and (b) (inner curves), randomly generated.

TABLE III

	Δb							
Δa	0	1	2	3	4	6	8	12
0	—	−0.00	−0.01	−0.02	−0.02	−0.04	−0.11	−0.15
1	−0.00	−0.01	−0.01	−0.02	−0.03	−0.05	−0.08	−0.15
2	−0.01	−0.02	−0.03	−0.03	−0.05	−0.07	−0.08	−0.12
3	−0.04	−0.05	−0.06	−0.06	−0.07	−0.08	−0.10	−0.13
4	−0.06	−0.06	−0.06	—	—	—	—	—

Relative errors of the analysis performed on a mixture of reference spectra affected by gain and offset drifts simulated during the acquisition process. The data base contains 16 spectra.

fore, be considered as not valid. The results become compatible with those found previously, thus proving the equivalence between both cases.

B. Analysis of Real Data

The data base was built up using 3 isotopes (^{133}Ba, ^{137}Cs and ^{60}Co), whose spectra were taken with a NaI detector and a MCA Camberra model 35PLUS. Calibrated sources (10 μCi placed 1 cm in front of the crystal) were used with exposure times ranging from 100 to 2000 min for both pure and mixtured samples. The spectra were taken at different instants of time and, therefore, there is non-null probability of appearing drifts between these last patterns and the reference ones.

In effect, several perturbations were clearly observed in the operation of the spectrometer. An example of them is plotted in Fig. 3. It consists of a mixture of ^{133}Ba and ^{137}Cs, whose pattern is represented together with the (mathematical) composition of the two reference spectra used to calibrate the algorithm. Such an important distortion in shape has a dramatic influence on the response that the standard Memory would offer: the shifting of the individual peaks exhibited in the composite spectrum is great enough to destroy the similarity between this last pattern and any linear combination of the reference ones.

However, the application of the extended memory, calibrated with the spectra corresponding to pure isotopes,

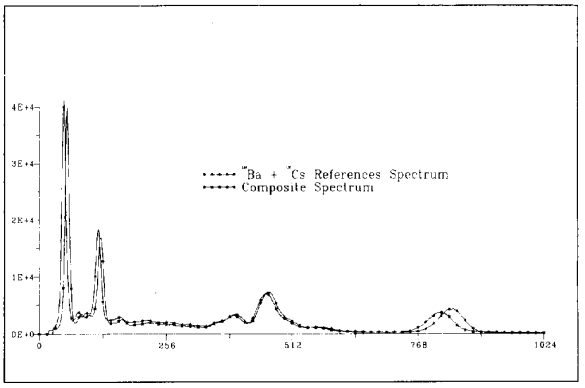

Fig. 3. Real spectrum of a mixture of ^{133}Ba and ^{137}Cs affected by drifts in the spectrometer, together with the spectrum constructed by means of the arithmetical addition of the calibration patterns.

leads to results as satisfactory as those shown in Table IV. The quantitative analysis of some of the considered spectra is given there, the numbers reflecting the errors in the concentration of each identified isotope (left column) in the spectra under analysis (top row). These last patterns have been formed by exposing the detector to the same sources used in the calibration, during periods of time whose ratios with respect to the times corresponding to the reference spectra are representing by the multiplicative coefficients of each isotope. The errors refer to the differences between the true concentrations of the components present in the samples (the multiplicative coefficients) and the ones obtained from the application of the algorithm, normalized to the actual contribution of each isotope. Drifts in gain and zero are also estimated, as well as the values of the rejection coefficients derived from the method. In all the cases analyzed, this last parameter has been kept low enough to consider the response as valid and the accuracy achieved in the isotope quantification becomes reasonably good (with errors lower than 15%),

TABLE IV

Ref. Spectra	Mixture						
	$1*^{133}Ba$	$1*^{137}Cs$	$1*^{60}Co$	$10*^{60}Co$	$1*^{133}Ba + 1*^{137}Cs$	$1*^{133}Ba + 1*^{137}Cs$	$10*^{60}Co$
^{133}Ba	+0.08	—	—	—	−0.05	−0.03	—
^{137}Cs	—	+0.01	—	—	−0.05	−0.15	—
^{60}Co	—	—	−0.11	−0.09	—	—	−0.12
Gain drift	−3.2%	−1.3%	−1.3%	+1.2%	+0.4%	+5.4%	−2.1%
Zero drift	+15	−0.3	−0.1	+2.7	+14.6	+14.2	+2.5
Rejection coef.	0.02	0.01	0.05	0.04	0.06	0.06	0.04

Results obtained in the analysis performed on the real (drifted) spectra. The patterns contained 2048 energy channels and the numbers refer to the relative errors obtained in the isotope quantification, as well as estimations of the gain and zero drifts.

even when the instrument is affected by relatively large drifts.

V. Conclusions

The performance of the automatic spectrum analysis based on the use of Associative Memory algorithms has been improved by introducing the capability of dealing with linear drifts in the nuclear instrumentation. This extension has been accomplished by augmenting the reference isotope base with the successive derivatives of the calibration spectra. Thus, the pseudo-inverse matrix is constructed at the beginning of the process with these data and no further mathematical computations are required during the operation, fact that simplifies greatly the required hardware support, making it compatible with a simple implementation both in PC or ASIC. For instance, the analysis shown in the last sections have been carried out in a PC386SX computer with a 387SX coprocessor. Essentially, the whole process is reduced to perform a matrix by a vector multiplication, operation that needs less than 1 s in the worst case. The longest process, i.e., the determination of the reference pseudo-inverse matrix, is done just once during the training phase.

The mathematical formulation of the method is based on the assumption of linearity between the photon energy and its associated channel number; however, this approximation becomes sufficient for those applications where extreme accuracy is not required. The examples shown in this paper confirm this fact. In future works, we will explore those cases in which nonlinear calibration-energy relationships (such as quadratic or other more complex expressions) are employed. The introduction of these functions in the formulation of the extended associative memory algorithms would make them useful to deal with drifts occurred in devices that present, for instance, the well known characteristics of nonlinearity in the lower channels of the spectrum.

VI. Acknowledgments

Authors wish to acknowledge the kind collaboration of the Institute of Studies of the Energy at CIEMAT in the acquisition of the experimental data exposed in this paper. Special thanks should be given to Dr. R. Gaeta, M. L. Marco and F. Navarro.

This work has been done in collaboration with AMYS, within the Spanish Electrotechnique Investigation Program (PIE), which is financed by the Spanish Electric Sector and coordinated by OCIDE.

References

[1] P. Olmos *et al.*, "A new approach to automatic radiation spectrum analysis," *IEEE Trans. Nucl. Sci.*, vol. 38, no. 4, pp. 971–975, 1991.

[2] P. Olmos *et al.*, "Applications of neural network techniques in gamma spectroscopy," Proceedings of the ICRM'91 Symposium. Madrid, May 1991, *Nucl. Instrum. Meth.*, vol. A312, pp. 167–173, 1992.

[3] M. Yamashita, "A pulser-controlled dual window unit for use in gain stabilization of scintillation detectors," *Nucl. Instrum. Meth.*, vol. 114, pp. 75–82, 1974.

[4] H. Holm, H. W. Fielding, and G. C. Neilson, "Gain stabilization of phototubes using a LED diode scheme," *Nucl. Instrum. Meth.*, vol. A234, pp. 517–520, 1985.

[5] D. C. Stromswold and J. E. Meisner, "Gamma-ray spectrum stabilization in a borehole probe using a Ligth Emiting Diode," *IEEE Trans. Nucl. Sci.*, vol. 26, no. 1, pp. 395–397, 1979.

[6] Z. Kosina, "Real time spectrum stabilization by software," *Nucl. Instrum. Meth.*, vol. 213, pp. 551–552, 1983.

[7] C. E. Cohn, "Improved stabilization schema for computerized pulse-height analyzers," *Nucl. Instrum. Meth.*, vol. 201, pp. 379–380, 1982.

[8] K. Debertin and R. G. Helmer, "Gamma- and X-Ray Spectrometry with Semiconductor Detectors," Amsterdam: North-Holland, 1988.

[9] T. Kohonen, *Self-Organization and Associative Memory*, New York: Springer-Verlag, 1988.